On Heliospheric Magnetic Field Reconstructions

Leif Svalgaard[1]

Corresponding author: Leif Svalgaard, W.W. Hansen Experimental Physics Laboratory, Stanford University, Cypress Hall C3, 466 Via Ortega, Stanford, CA 94305, USA. (leif@leif.org)

[1]HEPL, Stanford University, Stanford,
CA 94305, USA

Abstract. The paper "An analysis of heliospheric magnetic field flux based on sunspot number from 1749 to today and prediction for the coming solar minimum" by *Goelzer et al.* [2013], using the theory of *Schwadron et al.* [2010], is sought validated by comparison with an outmoded reconstruction of the heliospheric magnetic field (HMF). We suggest that a new analysis and revision of their paper based on comparisons with recent consensus reconstructions of the HMF would be a sharper test of the theory.

1. The Claim

Goelzer et al. [2013] using the theory of *Schwadron et al.* [2010] argue that magnetic flux is injected into interplanetary space by coronal mass ejection eruptions and removed by reconnection in the low solar atmosphere, producing a Heliospheric Magnetic Field intensity (HMF B) that is correlated with the sunspot number. They apply this theory to the sunspot record going back to 1749, claiming a favorably quantitative comparison with the results derived from ^{10}Be observations. Central to such a claim is that the HMF reconstruction used is as correct as possible or as we can make it. Unfortunately, the Goelzer et al. paper employs an outdated HMF reconstruction [*McCracken*, 2007] which is seriously at variance with HMF reconstructions published since 2007 based on geomagnetic data [*Svalgaard et al.*, 2003; *Svalgaard and Cliver*, 2010; *Lockwood and Owens*, 2011] as well as on cosmogenic nuclide data [*Steinhilber et al.*, 2010]. More recent work [*Lockwood et al.*, 2014; *Svalgaard*, 2014] confirms and extends the Steinhilber/Svalgaard/Lockwood consensus. Therefore, the quantitative conclusions reached by Goelzer et al. should be revisited and suitably revised. In addition, recent cosmic ray proxies of HMF B, [*Steinhilber et al.*, 2010], could be brought to bear.

2. The Reconstructions

Figure 1 shows the consensus reconstruction yearly average HMF B since 1845 compared with HMF B derived from the ^{10}Be cosmic ray proxy. The marked drop in cosmic ray proxy-based HMF B in 1953 and going back in time is due to an unsatisfactory splicing together of cosmic ray intensities derived from balloon-based calibrations of ion chamber records and neutron monitor data [after 1953]. To first order, the pre-1954 cosmic ray proxy-based HMF B is $\sim$2 nT too low throughout, as already pointed out by *Svalgaard and Cliver* [2010] (Figure 13 of that paper). Since this is a significant fraction (a third) of the average value of HMF B, conclusions (e.g. "compare favorably to the results derived from ^{10}Be observations") drawn from comparisons with the *McCracken* [2007] reconstruction are not warranted. Due to the inherent interest in and potential importance of the *Schwadron et al.* [2010] theory, we urge Goelzer et al. to repeat their analysis using up-to-date consensus HMF B reconstructions, both geomagnetic (published) and more recent cosmogenic isotope based (if released for publication).

Using the sunspot number as the ultimate input to their model makes sense as there is an [expected] correlation of the HMF B with the Sunspot Number (SSN), Figure 2, as noted by *Svalgaard et al.* [2003], *Svalgaard and Cliver* [2005], and *Karinen and Mursula* [2006]. The main sources of the equatorial components of the Sun's large-scale magnetic field are large active regions. As these to first order emerge at random longitudes, their net equatorial dipole moment will scale as the square root of their number. Thus their contribution to the average HMF strength will tend to increase as $SSN^{1/2}$ [*Wang and Sheeley*, 2003] as observed.The simple square root function of the SSN generally over-predicts slightly the HMF at the beginning of each cycle compared to the theory. The presence of widespread coronal holes during the declining phase of the cycle will generally increase HMF B over that predicted by sunspots at such times as duly observed.

Since the model used in *Schwadron et al.* [2010] has eight adjustable parameters it is not surprising [1] that a set of parameters (including a radial 'floor' of 56×10^{13} Wb) can be found that affords good agreement with HMF B derived from the observed OMNI dataset as well as from the reconstructions derived from the geomagnetic response, Figure 3. The parameters (typically uncertain by a factor of two) and the data used for the Figures can be found in the electronic supplement. All values are subject to minor corrections and adjustments as this rapidly evolving field of inquiry matures.

Acknowledgments. L.S. acknowledges the continuing support from Stanford University, and the stimulating impetus from the ISSI Team 233 discussions: `http://www.leif.org/research/Svalgaard_ISSI_Proposal_Base.pdf` as well as extensive advice and comments from the authors of *Goelzer et al.* [2013], including a spreadsheet (kindly provided by Nathan Schwadron) to run their model with user-specified parameters. In-situ data is obtained from the OMNI dataset at `http://omniweb.gsfc.nasa.gov/ow.html`.

Notes

1. von Neumann: "with four parameters I can fit an elephant, and with five I can make him wiggle his trunk", *Dyson* [2004].

References

Dyson, F. (2004), A meeting with Enrico Fermi, *Nature*, *427*, 297, doi:10.1038/427297a.

Goelzer, M. L., C. W. Smith, N. A. Schwadron, and K. G. McCracken (2013), An analysis of heliospheric magnetic field flux based on sunspot number from 1749 to today and prediction for the coming solar minimum, *J. Geophys. Res.*, *118(A12)*, 7525-7531, doi:10.1002/2013JA019404.

Karinen, A. and K. Mursula (2006), Correcting the Dst index: Consequences for absolute level and correlations, *J. Geophys. Res.*, *111(A8)*, A08207, doi:10.1029/2005JA011299.

Lockwood, M. and M. J. Owens (2011), Centennial changes in the heliospheric magnetic field and open solar flux: The consensus view from geomagnetic data and cosmogenic isotopes and its implications, *J. Geophy. Res.*, *116(A4)*, A04109, doi:10.1029/2010JA016220.

Lockwood, M., L. Barnard, H. Nevanlinna, M. J. Owens, R. G. Harrison, A. P. Rouillard, and C. J. Davis (2014), Reconstruction of Geomagnetic Activity and Near-Earth Interplanetary Conditions over the Past 167 Years: 3. Improved representation of solar cycle 11, *Ann. Geophys.*, (in press).

McCracken, K. G., Heliomagnetic field near Earth, 1428-2005 (2007), *J. Geophys. Res.*, *112(A9)*, A09106, doi:10.1029/2006JA012119.

Schwadron, N. A., D. E. Connick, and C. W. Smith (2010), Magnetic flux balance in the heliosphere, *Astrophys. J.*, *722*, L132-L136.

Steinhilber, F., J. A. Abreu, J. Beer, and K. G. McCracken (2010), Interplanetary magnetic field during the past 9300 years inferred from cosmogenic radionuclides, *J. Geophys. Res.*, *115 (A1)*, A01104, doi:10.1029/2009JA014193.

Svalgaard, L., E. W. Cliver, and P. LeSager (2003), Determination of interplanetary magnetic field strength, solar wind speed, and EUV irradiance, 1890-2003, in *Proceedings of ISCS 2003 Symposium: Solar Variability as an Input to the Earth's Environment, Eur. Space Agency Spec. Publ., ESA SP-535*, 15.

Svalgaard, L. and E. W. Cliver (2005), The IDV index: Its derivation and use in inferring long-term variations of the interplanetary magnetic field strength, *J. Geophys. Res.*, *110(A12)*, A12103, doi:10.1029/2005JA011203.

Svalgaard, L. and E. W. Cliver (2010), Heliospheric magnetic field 1835-2009, *J. Geophys. Res.*, *115(A9)*, A09111, doi:10.1029/2009JA015069.

93 Svalgaard, L. (2014), Errors in Scale Values for Magnetic Elements for Helsinki, *Ann. Geophys.*, *(in press)*.

95 Wang, Y.-M. and N. R. Sheeley Jr. (2003), On the fluctuating component of the Sun's large-scale magnetic field, *Astrophys. J.*, *590*, 1111, doi:10.1086/375026.

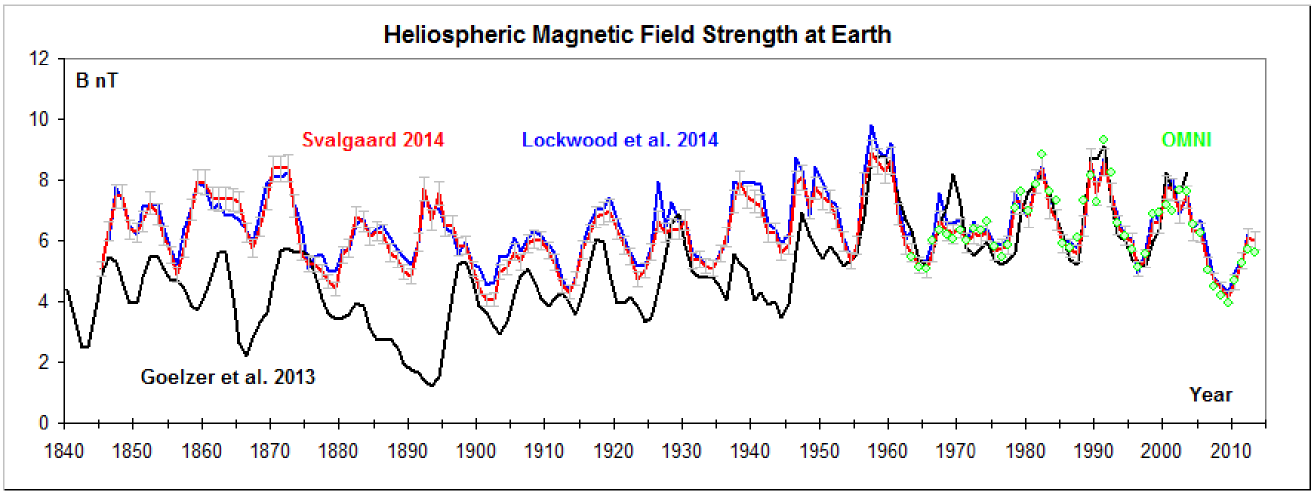

Figure 1. Reconstructions of the Heliospheric Magnetic Field (B in nanoTesla) at Earth: Blue curve from *Lockwood et al.* [2014]. Red curve from *Svalgaard* [2014] with conservative (grey) error bars. Green dots show yearly averages of B derived from the OMNI dataset `http://omniweb.gsfc.nasa.gov/ow.html`. *Goelzer et al.* [2013] compare their modeled field strength with data shown by the black curve derived from cosmogenic nuclide records by *McCracken* [2007].

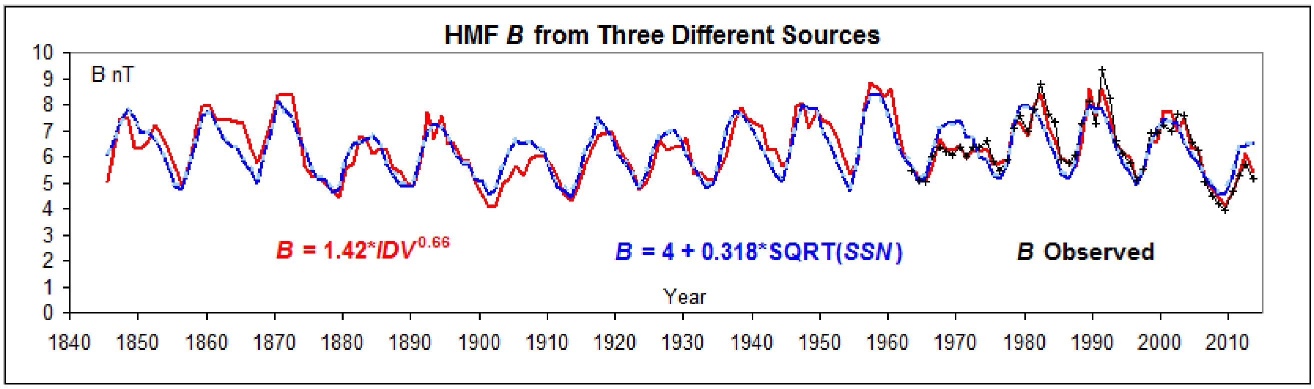

Figure 2. Reconstructions of the Heliospheric Magnetic Field (B in nanoTesla) at Earth: red curve is from a correlation ($R^2 = 0.89$) between OMNI B (1963-2013) and the IDV-index [*Svalgaard and Cliver*, 2005, 2010; *Svalgaard*, 2014]. The blue curve is derived from a correlation between the so derived B with the square root of the Sunspot Number (1845-2013, $R^2 = 0.73$; 1963-2013, $R^2 = 0.66$, dashed light blue overlay curve). The black curve with plusses shows yearly averages of B from the OMNI dataset.

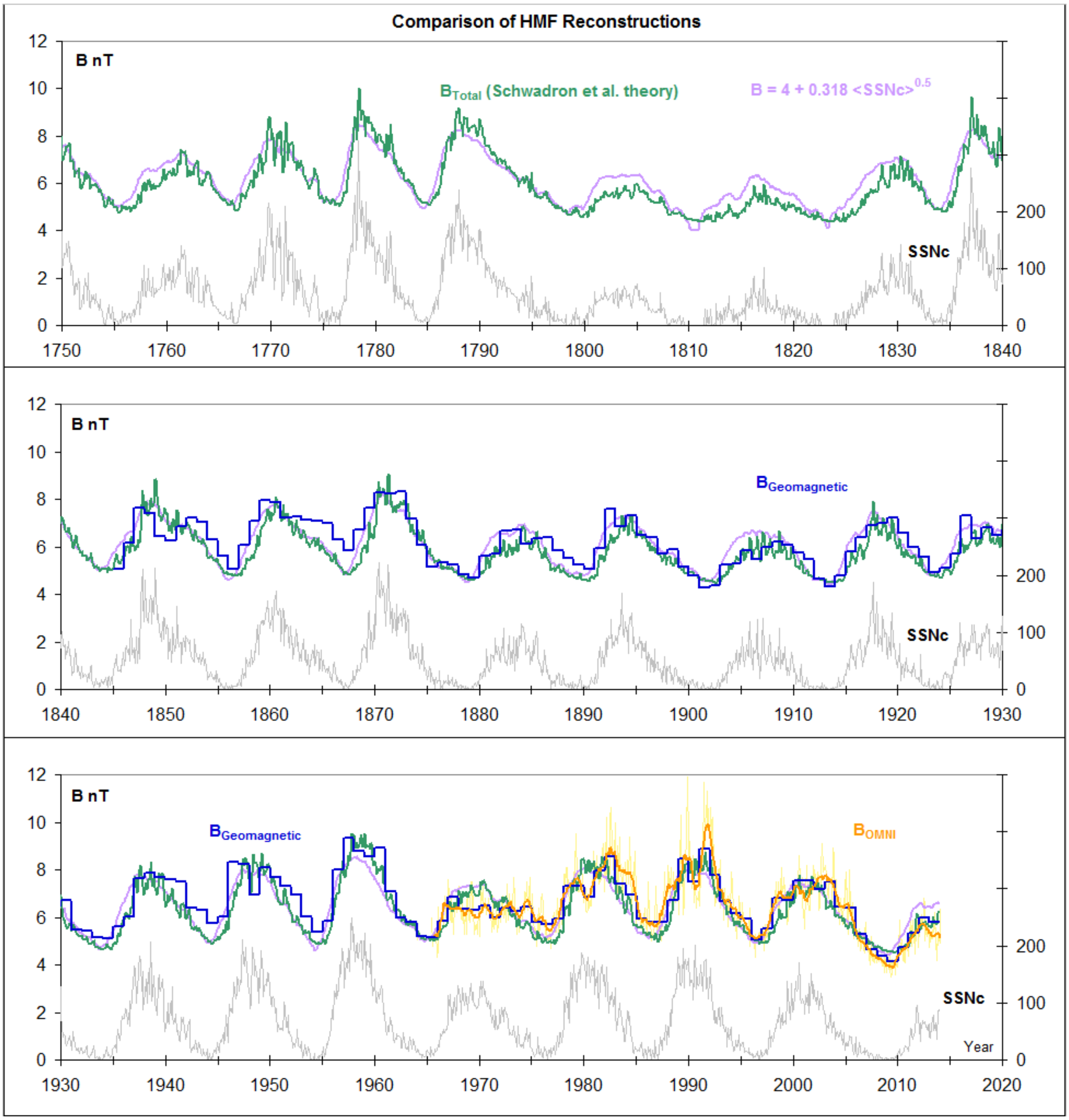

Figure 3. Comparison between HMF B derived from geomagnetic data (blue), from the 12-month average sunspot number using the relationship from Figure 2 (purple), and from the *Schwadron et al.* [2010] theory using the parameter set given in the supplementary data (monthly values in green). The OMNI 1-year central running average is shown in orange (27-day rotation averages in yellow).

Auxiliary material for
On Heliospheric Magnetic Field Reconstructions
Leif Svalgaard
Journal of Geophysical Research, Space Physics, 2014

Introduction.
The material consists of two files as explained below.

Explainer for
1. text01: Yearly values of Heliospheric Magnetic Field Strength.
1.1 Column "Year", the year.
1.2 Column "SSNc", the 'corrected' Sunspot Number. A preliminary synthesis of the SSN Workshop's reconciled sunspot number series [for details see http://www.leif.org/research/CEAB-Cliver-et-al-2013.pdf "Recalibrating the Sunspot Number (SSN): The SSN Workshops" (http://ssnworkshop.wikia.com/wiki/Home)].
1.3 Column "Geomagn", average of estimates by Svalgaard [2014] and Lockwood et al. [2014] expressed in nanoTesla.
1.4 Column "B(10Be)", the 10Be-based estimated HMF B in nT obtained by hand-digitizing Figure 4 in McCracken [2007].
1.5 Column "OMNI", yearly average total HMF B (nT) from the OMNI dataset. When possible, missing data for some years have been filled in by interpolation from data 27 days before and after.
1.6 Column "Theory", HMF B calculated from the Schwadron et al. [2011] theory, using an Excel spreadsheet kindly provided by Nathan Schwadron with the set of parameters given in 'text02' below.

Explainer for
2. text02: Parameters used in calculating HMF B.
2.1 Column "Svalgaard", the parameters used in this paper.
2.2 Column "Goelzer", the parameters used in Goelzer et al. [2013].
2.3 Column "Description", a short description of the parameter

Year	SSNc	Geomagn HMF B	B(10Be) McC2007	OMNI HMF B	Theory HMF B
1749.5	106.9		3.4		6.70
1750.5	118.4		3.2		7.23
1751.5	59.1		4.1		6.30
1752.5	54.8		4.9		6.11
1753.5	36.8		5.0		5.73
1754.5	16.3		4.5		5.18
1755.5	10.2		4.1		4.92
1756.5	17.4		4.0		4.95
1757.5	51.4		3.9		5.50
1758.5	63.9		3.8		5.87
1759.5	73.3		3.9		6.11
1760.5	84.7		3.9		6.45
1761.5	111.1		4.5		7.08
1762.5	79.1		4.4		6.56
1763.5	57.0		3.5		6.20
1764.5	42.0		2.6		5.89
1765.5	18.0		2.8		5.29
1766.5	12.3		3.7		5.01
1767.5	48.6		3.6		5.54
1768.5	92.0		3.2		6.37
1769.5	138.4		3.3		7.49
1770.5	134.0		3.5		7.72
1771.5	105.4		3.7		7.34
1772.5	83.0		4.7		7.00
1773.5	41.3		5.5		6.11
1774.5	40.5		5.5		5.95
1775.5	15.2		4.9		5.27
1776.5	21.5		4.7		5.19
1777.5	114.5		4.6		6.73
1778.5	195.8		4.0		8.81
1779.5	159.5		3.7		8.45
1780.5	110.4		3.7		7.76
1781.5	104.6		4.2		7.59
1782.5	48.9		4.5		6.45
1783.5	30.7		4.0		5.90
1784.5	9.3		3.7		5.25
1785.5	25.3		3.7		5.31
1786.5	112.0		4.3		6.77
1787.5	174.6		5.4		8.25
1788.5	162.0		5.7		8.54
1789.5	145.6		6.0		8.34
1790.5	112.8		5.8		7.90
1791.5	79.9		5.0		7.15
1792.5	75.2		4.3		6.76
1793.5	46.4		4.4		6.23
1794.5	51.8		3.9		6.13
1795.5	22.8		3.6		5.54
1796.5	24.6		3.1		5.38
1797.5	11.2		2.9		4.99
1798.5	6.4		2.6		4.76
1799.5	9.4		2.6		4.73

55	1800.5	21.4		2.8	4.84
56	1801.5	47.4		3.4	5.37
57	1802.5	49.6		4.1	5.52
58	1803.5	55.1		4.4	5.67
59	1804.5	51.5		4.2	5.66
60	1805.5	50.1		4.0	5.71
61	1806.5	26.4		3.5	5.26
62	1807.5	23.8		3.1	5.15
63	1808.5	6.9		2.6	4.73
64	1809.5	4.7		2.0	4.62
65	1810.5	0.0		1.5	4.44
66	1811.5	6.3		1.8	4.48
67	1812.5	12.3		2.4	4.56
68	1813.5	22.3		2.6	4.77
69	1814.5	16.4		2.5	4.70
70	1815.5	35.2		2.0	5.02
71	1816.5	52.3		1.6	5.50
72	1817.5	41.6		1.7	5.37
73	1818.5	29.3		2.4	5.16
74	1819.5	24.8		3.1	5.04
75	1820.5	16.1		3.5	4.88
76	1821.5	7.3		3.4	4.65
77	1822.5	5.5		3.1	4.55
78	1823.5	1.9		2.4	4.40
79	1824.5	8.7		2.2	4.53
80	1825.5	20.1		2.8	4.69
81	1826.5	40.6		3.7	5.09
82	1827.5	60.1		4.5	5.63
83	1828.5	80.8		5.7	6.15
84	1829.5	86.4		6.6	6.39
85	1830.5	91.8		6.7	6.61
86	1831.5	55.7		5.6	6.13
87	1832.5	30.4		3.8	5.54
88	1833.5	9.0		2.5	5.01
89	1834.5	14.8		2.7	4.93
90	1835.5	65.7		2.8	5.78
91	1836.5	151.5		2.6	7.45
92	1837.5	171.9		3.1	8.51
93	1838.5	122.2		4.4	7.82
94	1839.5	100.4		4.9	7.39
95	1840.5	72.7		4.5	6.83
96	1841.5	37.6		2.6	6.05
97	1842.5	24.9		2.6	5.60
98	1843.5	10.1		3.6	5.13
99	1844.5	14.6		4.9	5.03
100	1845.5	42.4	5.06	5.4	5.43
101	1846.5	67.8	6.16	5.3	5.96
102	1847.5	108.2	7.63	4.7	6.76
103	1848.5	146.0	7.42	4.0	7.72
104	1849.5	123.6	6.43	4.0	7.69
105	1850.5	83.1	6.24	4.9	6.99
106	1851.5	85.3	6.86	5.6	6.92
107	1852.5	70.7	7.20	5.5	6.65
108	1853.5	49.7	7.04	5.0	6.17

109	1854.5	23.4	6.30	4.8	5.52
110	1855.5	7.3	5.63	4.7	5.06
111	1856.5	4.9	5.05	4.5	4.81
112	1857.5	29.0	6.08	3.9	5.10
113	1858.5	65.4	7.06	3.8	5.80
114	1859.5	125.1	7.97	4.3	7.07
115	1860.5	138.7	7.84	5.0	7.61
116	1861.5	106.0	7.22	5.8	7.28
117	1862.5	73.1	7.28	5.7	6.73
118	1863.5	56.7	7.12	4.3	6.30
119	1864.5	55.2	7.08	2.8	6.18
120	1865.5	32.2	6.99	2.3	5.67
121	1866.5	20.2	6.31	2.9	5.30
122	1867.5	9.2	5.83	3.3	4.90
123	1868.5	43.0	6.70	3.7	5.40
124	1869.5	91.0	7.65	4.7	6.36
125	1870.5	170.1	8.26	5.7	8.05
126	1871.5	143.6	8.24	5.8	8.07
127	1872.5	123.6	8.31	5.6	7.78
128	1873.5	77.5	7.19	5.7	7.01
129	1874.5	51.6	6.08	5.6	6.37
130	1875.5	20.3	5.15	4.9	5.60
131	1876.5	12.1	5.34	4.1	5.21
132	1877.5	12.1	5.25	3.7	5.03
133	1878.5	3.5	4.84	3.6	4.73
134	1879.5	6.0	4.71	3.5	4.65
135	1880.5	33.8	5.62	3.7	5.09
136	1881.5	61.9	5.70	4.0	5.68
137	1882.5	64.5	6.67	3.9	5.88
138	1883.5	69.8	6.70	3.3	6.02
139	1884.5	78.3	6.14	2.7	6.36
140	1885.5	61.8	6.34	2.8	6.11
141	1886.5	29.5	6.37	2.9	5.48
142	1887.5	15.7	5.85	2.5	5.07
143	1888.5	8.7	5.54	2.0	4.85
144	1889.5	7.2	5.24	1.8	4.71
145	1890.5	8.4	5.04	1.7	4.64
146	1891.5	43.9	5.92	1.5	5.24
147	1892.5	85.9	7.60	1.2	6.13
148	1893.5	106.3	6.84	1.5	6.73
149	1894.5	95.7	7.31	2.7	6.81
150	1895.5	75.3	6.47	4.3	6.47
151	1896.5	46.9	6.37	5.4	5.97
152	1897.5	31.0	5.70	5.3	5.56
153	1898.5	29.0	5.89	4.6	5.42
154	1899.5	13.4	5.14	4.0	5.02
155	1900.5	10.4	4.80	3.6	4.85
156	1901.5	3.0	4.30	3.2	4.61
157	1902.5	5.0	4.36	3.0	4.55
158	1903.5	25.7	5.24	3.4	4.85
159	1904.5	48.8	5.29	4.3	5.36
160	1905.5	67.5	5.86	4.9	5.82
161	1906.5	61.2	5.47	5.1	5.84
162	1907.5	68.5	5.99	4.7	6.08

163	1908.5	56.0	6.21	4.1	5.88
164	1909.5	48.4	6.09	3.9	5.73
165	1910.5	21.5	5.77	4.1	5.27
166	1911.5	7.2	5.46	4.3	4.84
167	1912.5	4.0	4.64	3.9	4.65
168	1913.5	1.6	4.32	3.6	4.52
169	1914.5	11.2	4.78	4.3	4.60
170	1915.5	50.9	5.79	5.4	5.36
171	1916.5	66.4	6.42	6.1	5.77
172	1917.5	121.0	6.90	5.9	6.88
173	1918.5	93.9	6.97	4.9	6.80
174	1919.5	73.4	7.20	4.0	6.47
175	1920.5	42.2	6.57	3.9	5.85
176	1921.5	28.2	6.00	4.2	5.48
177	1922.5	15.4	5.56	3.9	5.12
178	1923.5	6.6	4.94	3.3	4.82
179	1924.5	18.0	5.09	3.5	4.90
180	1925.5	50.5	5.68	4.4	5.39
181	1926.5	72.8	7.29	5.6	6.03
182	1927.5	82.0	6.35	6.7	6.36
183	1928.5	90.4	6.83	6.7	6.59
184	1929.5	74.0	6.50	6.9	6.32
185	1930.5	41.8	6.69	5.9	5.89
186	1931.5	24.5	5.45	5.0	5.38
187	1932.5	12.8	5.42	4.9	5.03
188	1933.5	6.1	5.18	4.9	4.79
189	1934.5	10.0	5.09	4.8	4.72
190	1935.5	42.3	5.62	4.5	5.23
191	1936.5	94.7	6.03	4.1	6.28
192	1937.5	140.5	7.64	5.7	7.53
193	1938.5	130.4	7.86	5.4	7.57
194	1939.5	109.9	7.69	5.1	7.42
195	1940.5	79.6	7.60	4.1	6.81
196	1941.5	52.6	7.50	4.4	6.30
197	1942.5	34.6	6.41	4.0	5.81
198	1943.5	16.8	6.32	4.1	5.31
199	1944.5	10.3	5.76	3.4	4.99
200	1945.5	36.2	6.02	3.9	5.36
201	1946.5	105.9	8.31	5.8	6.58
202	1947.5	158.3	8.23	7.1	7.96
203	1948.5	142.1	6.96	6.3	7.93
204	1949.5	141.9	8.08	5.9	8.15
205	1950.5	82.9	7.67	5.5	7.20
206	1951.5	64.9	7.31	5.9	6.67
207	1952.5	30.6	6.96	5.7	5.87
208	1953.5	13.9	6.03	5.2	5.36
209	1954.5	4.5	5.38	5.5	4.94
210	1955.5	37.4	5.83	5.6	5.33
211	1956.5	137.4	8.01	6.8	7.21
212	1957.5	186.0	9.34	8.8	8.52
213	1958.5	192.6	8.80	8.9	9.15
214	1959.5	161.8	8.53	8.8	8.88
215	1960.5	108.8	8.94	8.4	7.93
216	1961.5	51.9	7.11	7.6	6.73

217	1962.5	34.7	5.96	6.8		6.12
218	1963.5	25.9	5.99	6.4	5.45	5.70
219	1964.5	10.5	5.26	5.5	5.12	5.20
220	1965.5	14.5	5.21	5.3	5.06	5.08
221	1966.5	44.6	5.78	5.6	6.00	5.48
222	1967.5	96.0	7.10	6.6	6.36	6.49
223	1968.5	105.3	6.44	7.2	6.19	6.92
224	1969.5	104.2	6.41	8.2	6.05	7.06
225	1970.5	112.5	6.55	7.2	6.35	7.32
226	1971.5	72.1	5.94	6.5	6.00	6.63
227	1972.5	72.4	6.42	6.0	6.38	6.62
228	1973.5	38.5	6.19	5.8	6.35	5.90
229	1974.5	34.4	6.36	5.6	6.63	5.65
230	1975.5	15.6	5.78	5.5	5.82	5.19
231	1976.5	13.4	5.82	5.3	5.45	4.99
232	1977.5	29.5	5.99	5.5	5.85	5.16
233	1978.5	102.3	7.42	5.6	7.08	6.49
234	1979.5	155.4	7.16	6.9	7.59	7.78
235	1980.5	154.6	6.77	7.6	6.98	8.16
236	1981.5	140.5	8.04	8.0	7.84	8.12
237	1982.5	115.9	8.42	8.3	8.81	7.80
238	1983.5	66.8	7.26	7.6	7.61	6.90
239	1984.5	45.7	6.73	6.8	7.32	6.28
240	1985.5	18.0	5.99	6.2	5.89	5.52
241	1986.5	13.4	5.85	5.5	5.74	5.22
242	1987.5	29.4	5.67	5.3	6.09	5.32
243	1988.5	100.2	6.43	6.8	7.30	6.48
244	1989.5	157.6	8.60	8.8	8.15	7.96
245	1990.5	142.6	7.61	8.8	7.29	8.01
246	1991.5	145.7	8.63	9.1	9.34	8.21
247	1992.5	94.3	7.52	7.2	8.25	7.43
248	1993.5	54.6	6.68	6.2	6.59	6.56
249	1994.5	29.9	6.13	6.0	6.15	5.87
250	1995.5	17.5	6.00	5.5	5.73	5.42
251	1996.5	8.6	5.01	5.4	5.11	5.04
252	1997.5	21.5	5.54	5.3	5.54	5.09
253	1998.5	64.3	6.78	6.0	6.89	5.83
254	1999.5	93.3	6.61	6.4	6.91	6.51
255	2000.5	119.6	7.73	8.3	7.19	7.19
256	2001.5	111.0	7.86	7.6	6.96	7.18
257	2002.5	104.0	6.92	8.3	7.64	7.26
258	2003.5	63.7	7.47	6.9	7.60	6.51
259	2004.5	40.4	6.39	5.8	6.53	5.97
260	2005.5	29.8	6.48		6.25	5.58
261	2006.5	15.2	5.41		5.03	5.20
262	2007.5	7.5	4.74		4.48	4.89
263	2008.5	2.9	4.47		4.21	4.67
264	2009.5	3.1	4.23		3.93	4.55
265	2010.5	16.5	4.78		4.67	4.74
266	2011.5	55.7	5.38		5.25	5.42
267	2012.5	57.7	6.15		5.71	5.69
268	2013.5	64.9	6.00		5.16	5.84

Svalgaard	Goelzer	Unit	Description
0.04	0.04	Number	Number of CMEs per day per unit sunspot number
0	0	Number	Offset in calculating ejection frequency = offset + CMEs per day * Sunspot Number
15	20	Days	Timescale for interchange reconnection
4.0	2.5	Years	Timescale for opening of closed flux
3.0	6.0	Years	Timescale for loss of flux by disconnection
1	1	10^13 Wb	Magnetic flux per CME
56	0	10^13 Wb	Magnetic flux over whole sphere for a Floor in the HMF radial B
0.6	0.5	Fraction	Fraction of flux closing on ejection
1.5	N/A	Factor	Factor to convert computed, ideal 'Parker' spiral B to messy, total B
N/A	0.5-2.4	nT	Offset to convert computed, ideal 'Parker' spiral B to messy, total B